



BETTER SHIPS, BLUE OCEANS

Trade-off between URN and GHG in propeller design

Report No. : 77002-2-RD
Date : March 2025
Version : 1.0
Final Report

Trade-off between URN and GHG in propeller design

MARIN order No. : 77002.700
MARIN Project Manager : Johan Bosschers

Number of pages : 34

Ordered by : Ministry of Infrastructure and water management
Directorate-General for Aviation and Maritime Affairs
Rijnstraat 8
2515 XP The Hague
The Netherlands

Reported by : E.J. Foeth
Reviewed by : J. Bosschers

Version	Date	Version description	Checked by
1.0	07-03-2025	Final	J. Bosschers

CONTENTS	PAGE
REVIEW OF TABLES AND FIGURES	III
MANAGEMENT SUMMARY	IV
1 INTRODUCTION.....	1
1.1 Appraisal of SDC9/INF.11	2
2 PROPELLER DESIGN METHODOLOGY	3
2.1 Wake field	3
2.2 Geometry	4
2.3 Optimisation process	6
2.4 Analysis tool and cavitation	7
2.5 Estimation of noise levels	10
3 TRADE-OFF BETWEEN URN AND GHG	12
3.1 Results of the propeller design study	12
3.2 Effect of slow steaming and propeller design	16
3.3 Revisiting SDC9/INF.11	19
4 CONCLUSIONS AND RECOMMENDATIONS	25
REFERENCES	27

REVIEW OF TABLES AND FIGURES

Tables:

Table 3-1 - Selected properties of propellers 1 to 6 at a service speed of 18 knots.	15
---	----

Figures:

Figure 2-1 - Calculated nominal wake field, full scale, axial and in-plane components.....	3
Figure 2-2 - Rear view of a right-handed propeller (reference frame, selected terminology).	4
Figure 2-3 - Sectional definitions, II.....	4
Figure 2-4 - Blade outline plots showing the effect of various parameters,	5
Figure 2-5 - Optimisation design cycle.....	7
Figure 2-6 - Cavitation on a model propeller taken in MARINs testing facilities.	8
Figure 2-7 - Typical results of an estimated total propeller source level and its constituents as a power spectrum (decade bandwidth levels). Some contributions (here: face-side sheet and tip vortex) do not appear.	11
Figure 3-1 - Full optimisation progression.....	13
Figure 3-2 - Optimisation progression, Pareto-front close-up, plus 6 propellers selected for further study.	13
Figure 3-3 - 3D renderings of propellers 1 to 6.	14
Figure 3-4 - Various RNL metrics along the Pareto Front, ship speed 18 knots.	15
Figure 3-5 - RNL for the six propellers at the ship design speed. The black and red line denote the DNV SILENT-E transit and quiet class notations, respectively.....	17
Figure 3-6 - Close-up of Figure 12, 63 and 125 Hz centre frequency location indicated by vertical black lines.	17
Figure 3-7 - Overall RNL as a function of ship speed, separately showing the contribution of the machinery, tip vortex and attached cavitation, for propellers 1 (blue) and 6 (green).	18
Figure 3-8 - As Figure 3-6, showing overall Ship noise only and two assisting lines $RNL \propto \log_{10} V_S^{pow}$ for exponents 2.5 and 6.	18
Figure 3-9 - Ship speed as a function of voyage duration for various track ratios, assuming the ship sails 14.5 knots in the quiet zone.....	19
Figure 3-10 - Computed speed-power relation for all six propeller designs using model test results	19
Figure 3-11 - Margin against exceeding assumed RNL limits in dB in the quiet zone as a function of ship speed and efficiency relative to the most efficient propeller.....	20
Figure 3-12 - Increased ship speed outside quiet zone as a function of the track ratio.	21
Figure 3-13 - ORNEL vs track ratio, propellers 1 to 6.....	21
Figure 3-14 - Relative fuel use as a function of track ratio, all propellers	22
Figure 3-15 - Relative fuel use as a function of track ratio, propellers 1-4	23
Figure 3-16 - Relative fuel use as a function of track ratio, propellers 1, 5, 6.....	23

MANAGEMENT SUMMARY

Anthropogenic underwater noise has increased significantly since the industrial revolution and is negatively affecting the marine soundscape (Duarte et al. 2021). Shipping noise is recognised the most ubiquitous and pervasive source with effects on marine life ranging from changes in behavioural response, masking of communication and echolocation, and stress (Erbe et al. 2019).

In this report was a propeller design optimisation study for a single container vessel was performed exploring the balance between fuel consumption and underwater radiated noise using the latest noise estimation models. A range of propeller designs was found whereby a reduction in noise would always result in an increase of fuel use (for the same ship speed).

In November 2022 Japan submitted their document (SDC 9/INF.11 2022) to the IMO. This study was repeated here using the propellers obtained from the optimisation study.

In both studies it was assumed that the ship sails through a quiet region where a given noise limit may not be exceeded. The quieter propeller, the smaller the required slowdown. If no delays in arrival time are allowed than the loss of time due to the slowdown require an increase in service speed compared to the most efficiency & 'loudest' reference propeller. When the slowdown occurs over 10-20% of the total track length of the ship (or more), then propellers that are 2 to 4% less efficient than the reference propeller where found to have an overall lower fuel use as a consequence of having a lower required service speed outside the quiet region.

The conclusions qualitatively support SDC9/INF.11, although in the current study the break even point in fuel use was found at smaller sizes of the quiet region by virtue of the propeller optimisation strategy being able to achieve its goals at only half the propeller efficiency losses as reported in SDC9/INF.11

1 INTRODUCTION

Anthropogenic underwater noise has increased significantly since the industrial revolution and is negatively affecting the marine soundscape (Duarte et al. 2021). Shipping noise is recognised the most ubiquitous and pervasive source with effects on marine life ranging from changes in behavioural response, masking of communication and echolocation, and stress (Erbe et al. 2019). Within the International Maritime Organization (IMO), revised guidelines¹ for the reduction of underwater noise from commercial shipping to address these adverse impacts on marine life has been approved in July 2023 (MEPC.1/Circ.833). Operation solutions are available such as rerouting, slowing down (Findlay et al. 2023; A. O. MacGillivray et al. 2019). Technical solutions are available using e.g., low-noise propeller design or air injection (Lloyd, Foeth, et al. 2024). This reports focusses a technical solution by means of propellers designed for low noise. The (operational) effects and modelling of slowing down on noise are discussed in part two of this study in MARIN report 77002-3-RD.

In November 2022 Japan submitted their document (SDC 9/INF.11 2022) to the IMO, reporting on a study on the effect of propeller design with varying noise levels and efficiencies on overall fuel use, and thereby directly on greenhouse gas (GHG) emissions. It was postulated that a ship sailing through regions with a noise restriction would incur a speed reduction to meet said restrictions, and that this temporary slowdown would be later compensated by a speed increase to maintain the arrival time. A less efficient propeller would be quieter and the ship can then sail both faster in the region with a noise restriction and need not sail much faster outside that region, compared to a vessel equipped with a more efficient (noisier) propeller. The study showed that when the track length of the noise-restricted area is comparatively small that the net fuel use of the quieter but less efficient propeller exceeds that of the efficient design. When the region is around 25-30% of the total track the more quiet propeller has a lower overall fuel consumption, and, when the region is around 30-40% of the total track the slowdown of the most efficient propellers required the ship to exceed its maximum ship speed outside that region; the ship can no longer arrive on time.

¹ with respect to 2014

1.1 Appraisal of SDC9/INF.11

The document SDC9/INF.11 was received with interest by I&W who in their turn requested MARIN to study its contents, confirm its findings and extend the applied methods where necessary. It was observed by MARIN that in the study in SDC9/INF.11 that:

- While the blade-area ratio of the propellers was varied, to what extent the blade geometry was adapted (and within which constraints) and to what extent these designs were fully optimised for low noise was not apparent.
- The sound was estimated using Brown's model (Brown 1976) that uses the estimated attached cavitation extent; however, this is not the only form of cavitation that contributes to propeller noise. The contribution of the propeller's (cavitating) tip vortex was not included and this contribution often dominates. Furthermore, no machinery noise was included; when no attached or tip vortex cavitation is present then this noise source will remain.

The machinery noise is weakly dependent on ship speed, and above a certain ship speed the contribution of the cavitation, specifically tip vortex noise, may increase strongly. Adding these two contributions might lead to different conclusion in terms of noise as a function of ship speed. The study was hence repeated addressing the above observations, utilising the two latest developments in low-noise propellers design, namely:

- Application of multi-objective optimisation algorithms coupled to a fully flexible geometry description allowing for a thorough exploration of the propeller design space constrained by industry-standard design guidelines.
- Application of noise estimation functions for the sheet cavity, appended by the contribution of the cavitating tip vortex and of the machinery, using the latest available models.

In SDC9/INF.11 a 5500 TEU container ship was selected as a subject. This ship operates at 18 knots service speed with a maximum speed of 21.5 knots. The subject of the case study reported here is a 9000 TEU vessel container ship recently tested for its performance at MARIN's facilities and of which the ship wake field and other design data was allowed to be used by the prospective owner. This ship was also designed for a 18 knots service speed with a maximum speed of 20.0 knots.

The general methodology of propeller design and its various aspects is discussed briefly in Chapter 2 including a description of the various noise models used. The trade-off between noise and net fuel use is discussed in Chapter 3.

2 PROPELLER DESIGN METHODOLOGY

This section presents an introductory overview of the propeller optimisation procedure required to obtain industry standard propeller designs and an overview on the models used to estimate the underwater radiated noise of a ship.

2.1 Wake field

One of the key drivers of the propeller loading variations and cavitation response is the flow field behind the hull at the location of the propeller plane; the wake field (Figure 2-1). This wake field shows the velocity distribution at the location of the propeller disk following from a calculation of the flow around the hull of the ship at the design speed, including the effect of its own waves, trim and sinkage of the hull. The colour scale indicates the axial velocity while the velocities in the propeller plane are plotted as arrows—generally an upwards directed velocity as the flow follows the hull—all with reference to the ship speed.

The minimum axial flow velocity locally reaches values of only half the ship speed; here one expects an increase in the angle of attack and increase in blade loading to its highest value. Assuming the propeller to be right-handed; as a blade rotates upwards from the 9 o'clock towards the 12 o'clock position the in-plane velocity components are with the direction the rotation, and when the blade passes the 12 o'clock position these components are against the direction of rotation; these effects will lead to under and overloading conditions respectively. The underloading condition can lead to cavitation on the face side—the propeller side when viewing the vessel from behind—and overloading can lead to cavitation on the back side. Fixed pitch propellers are typically designed to be free of face-side cavitation, as the erosion risk is higher and the dynamic behaviour of face-side cavitation does not allow for the same degrees of freedom in the propeller design as back-side cavitation. The variations in e.g., ship speed, engine power, operational conditions and required thrust, combined with the topology of the wake necessitate a custom propeller design to manage cavitation for each new ship.

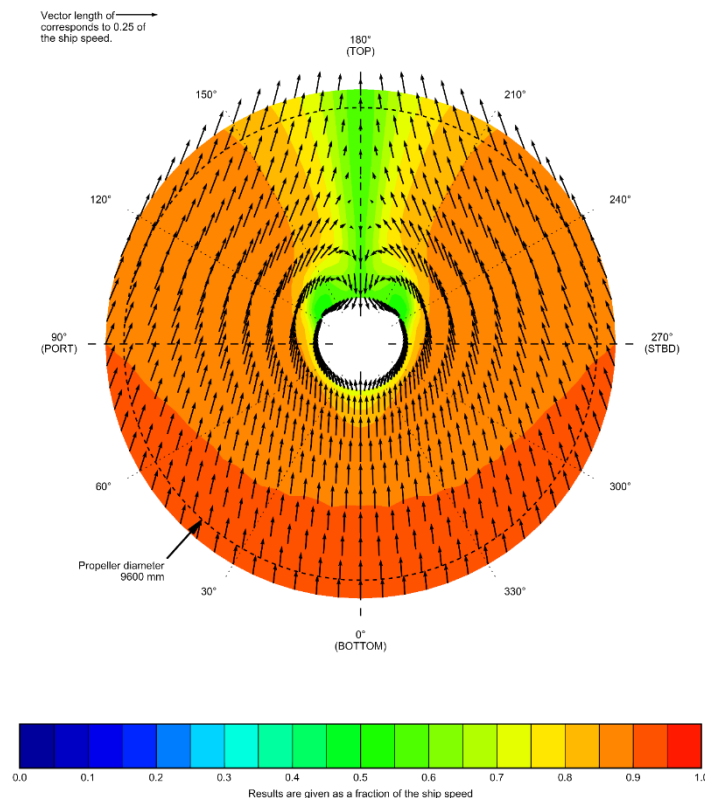


Figure 2-1 - Calculated nominal wake field, full scale, axial and in-plane components.

2.2 Geometry

For the optimisation a straightforward and intuitive geometric description propeller is used, typically in a polar reference frame, Figure 2-2. The propeller is built up from a series of sections—or hydrofoils—each defined on a cylinder of constant radius. A series of six radial distribution curves are used to define the main properties of the section: the position of the mid-chord point of each section, its pitch angle and chord length are used to manipulate the section position and rotation on the cylinder surface.

The sectional outline is built up from a mean thickness and a mean offset in terms of the value at y along the chordwise position x , see Figure 2-3. These distributions are referred to as the *sectional* thickness and camber distributions; the *radial* thickness and camber distribution are the maximum values of each individual section at each radial position along the propeller blade span, used for scaling the sections.

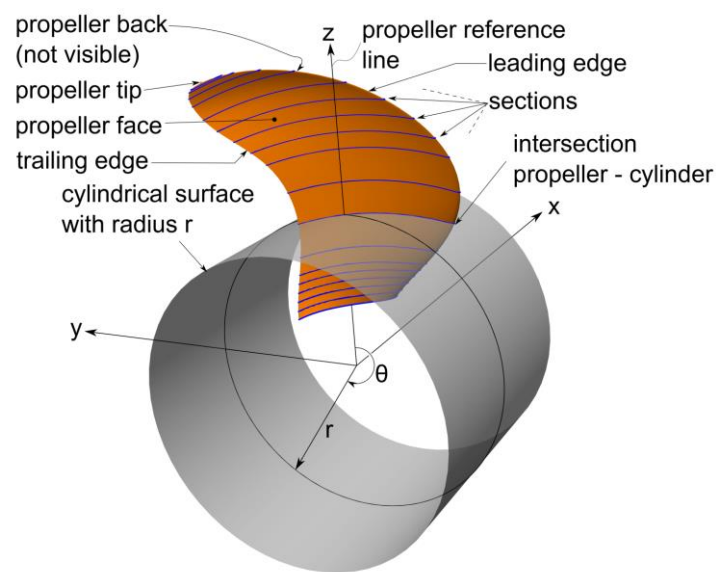


Figure 2-2 - Rear view of a right-handed propeller (reference frame, selected terminology).

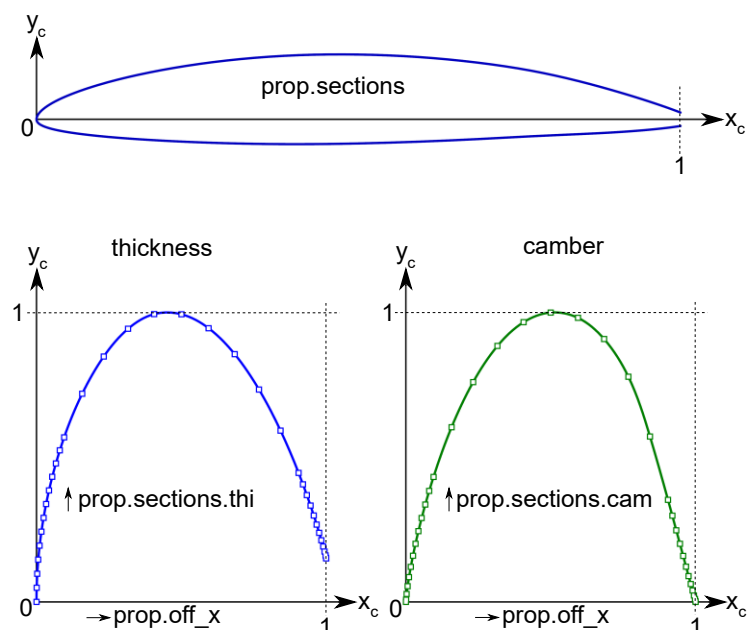


Figure 2-3 - Sectional definitions, II.

All the radial distributions and the sectional distributions were described by 3rd to 5th order Bézier curves, e.g. (Sederberg 2016), whereby the location of the control points of these curves could be moved either directly, or, were described by some empirical function tailored towards amenable distributions for propeller design. For example, the parameterised blade outline is given in Figure 2-4 that is a function of five parameters that steer the control points in order to obtain ‘outline-like’ curves preferred by designers.

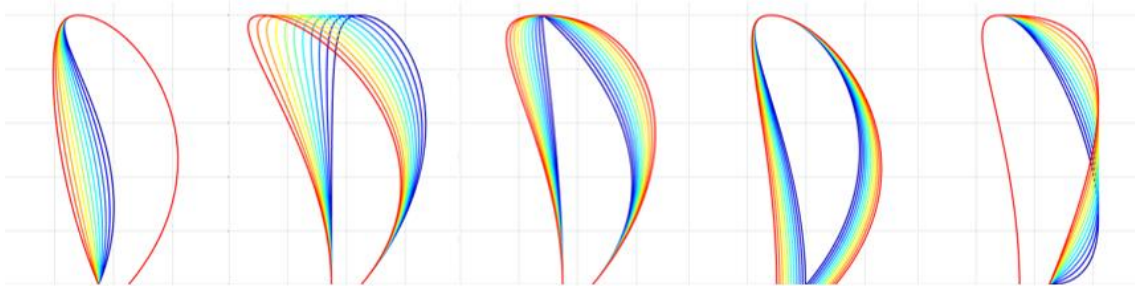


Figure 2-4 - Blade outline plots showing the effect of various parameters.

The hydrofoil geometry is also allowed to vary during the optimisation and no standard hydrofoils were used as is common for more traditional design. The section thickness of the hydrofoils was described fully parametrically (Foeth and Deij-van Rijswijk 2019) using six parameters whereby—amongst others—the leading edge geometry can be directly prescribed, as this is an important parameter to tune cavitation inception (Valentine 1974). Each parameter of the sectional camber and thickness was a smooth function with the propeller radius giving a unique section at each radial station. For the current study a total of 33 geometric parameters describe the blade geometry.

2.3 Optimisation process

Our first task is the design of a range of propellers optimised for high efficiency - leading to a lower use, reduced fuel consumption and therefore low green-house gases (GHG) emissions assuming the main engine does not use fuels from a renewable source-and low underwater radiated noise (URN). It has been well established that cavitation is an important contributor to the ship URN and that designing for well-behaved cavitation acts as a constraint on the design space: GHG and URN may be conflicting demands. To this end we use multi-objective optimisation algorithms. These algorithms have two major advantages over a more traditional design method whereby a single design is iteratively adapted by an experienced designer:

1. Modern algorithms can automatically search the entire design space and find the propellers with the best performance within the parameters set by the designer.
2. When the goals are conflicting then modern algorithms will not find a single solution, but an entire range of solutions; for each solution making one goal better will always make another goal worse. This trade-off is called the Pareto-optimal solution.

A propeller design framework PropArt, developed at MARIN, was used for the entire workflow. This framework is used on a daily basis whereby (typically) propeller efficiency is balanced by two forms of cavitation hindrance: onboard noise and vibration, and, cavitation erosion risk. Presently, for commercial applications, underwater radiated noise is usually not taken into account and when a ship does need to be silent, the Cavitation Inception Speed (CIS)—the speed at which any form of cavitation first occurs—is a design requirement. These designs nearly always require custom hydrofoil sections—tailored for optimal interaction between the flow pattern from the hull and loading of the propeller. Above the CIS these propellers may have a high erosion risk and these propellers are also known to be less efficient. For the current study we intend to arrive at a more subtle balance and do not design for a high CIS (per se) and we do not accept a high cavitation erosion risk (constraints are detailed below).

The general optimisation cycle is shown in Figure 2-5. The geometry is described by functions as described above. For each propeller any number of so-called preflight functions follow that may either accept, reject, or modify the geometry; these functions usually follow from an analysis of the (geometric) parameters alone. For instance, propellers may be rejected if they do not fall within a certain mass range of the blades (here: no more than 60 tons), or, if they are not compliant with classification society scantling rules. Propellers rejected upon creation can be automatically replaced before submitting the calculations to our computational cluster used to evaluate each new generation of designs. When a new generation is created an iterative setpoint iteration routine follows: all propellers are required to meet our operational design point—the specific thrust at a design speed and shaft rate of revolutions—which is typically not met for a new design candidate. An iterative loop is used whereby the propeller pitch distribution is scaled to meet that point, alleviating the optimiser from satisfying a constraint that can be easily corrected for. The pitch is adapted using a series of (time-averaged & fast) steady flow calculations in a circumferentially averaged wake field, and followed by fully unsteady flow simulations; the preflight functions are re-applied at each iterative step and only now our corrected geometry is ready for detailed analysis. After this analysis all goals & constraints are evaluated, and compared to the previous generation. When any constraint is violated an individual is said to be infeasible.

For our optimiser we selected the Competitive Multi Objective Particle Swarm algorithm (CMOPSO) by Zhang et al. (Zhang et al. 2018) that outperformed the other methods tested for our application, including the benchmark genetic algorithm (GA) NSGA-II algorithm (Deb et al. 2002). The CMOPSO method was modified to handle constraints by using the “parameterless method” (Deb 2000), thereby always favouring feasible over infeasible individuals in its Pareto-ranking procedure.

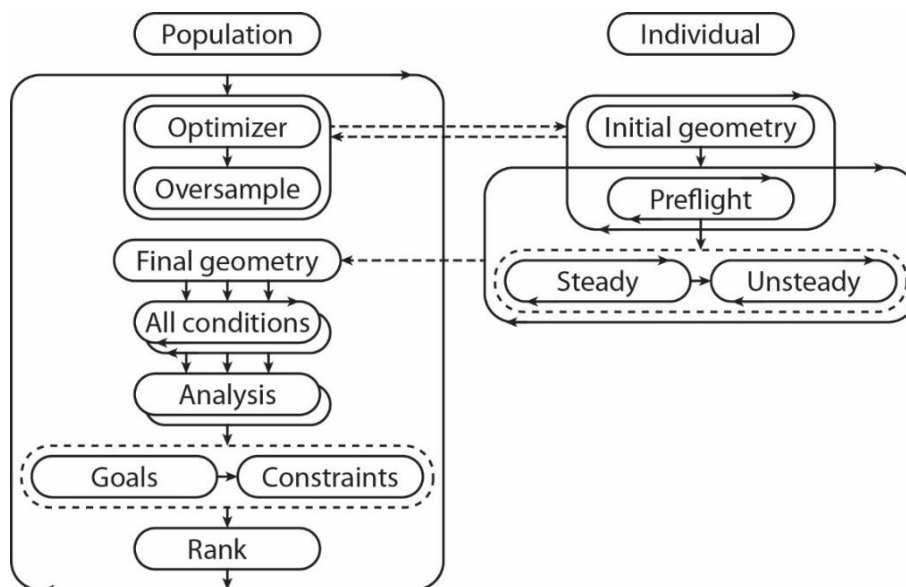


Figure 2-5 - Optimisation design cycle.

2.4 Analysis tool and cavitation

The propeller analysis method used is PROCAL, a boundary-element method (BEM) developed with the MARIN Cooperative Research Ships programme (Vaz and Bosschers 2006). A BEM is an inviscid method meaning that not all flow details are fully resolved, but is well able to reliably calculate the propeller performance—including an analysis of the cavitation—within about half an hour on a single CPU core. This fast turn-around time makes the code ideally suited for day-to-day design work, or, the analysis of large families of designs on our computational cluster with the entire optimisation process running for a few days.

The main cavitation noise sources are typically attached (or sheet) cavitation and tip vortex cavitation. In Figure 2-6 an image taken in MARIN's facilities shows a cavitating propeller with the attached cavity on the blade surface of blade 1 (12 o'clock position); a cavitating vortex is observed trailing in the wake of blade 4. The blade-rate effect of sheet cavitation in the near-field region of the propeller has been identified as the main contributor of low-frequency propeller-induced force fluctuations on the hull leading to onboard noise and vibration. The effect can be roughly divided as the flow displacement of blade and cavity thickness leading to a rotating pressure disturbance over the hull, blade loading (variations) and, the dynamics of the cavity volume with a monopole-like pressure-radiating behaviour. The latter effect constitutes a far more effective mechanism to excite the hull and is heavily influenced by the loading variation of the blade as it rotates through the ship's wake, and, will contribute to the blade-rate frequencies of the far-field URN. For most ships the attached cavity on the back side is present in the regions of lowest inflow velocity, either in the boundary layer from the hull of a single-screw vessel, or, wake of the shaft line of a twin-screw vessel. Besides being a source of both onboard and noise, cavitation can be highly erosive to the propeller blade surface or the ship's rudder.



Figure 2-6 - Cavitation on a model propeller taken in MARINs testing facilities.

One particularly erosive form of cavitation is bubble cavitation that occurs in regions where the pressure gradually falls below the vapor pressure; nuclei/small bubbles in the flow rapidly expand to larger bubble size and later collapse typically on or near the material surface. The region of gradual pressure gradients where bubble cavitation is often the mid-chord region of the blade. Bubble erosion risk constraints can be obtained from the results of an analysis by PROCAL using a fully wetted—i.e., non cavitating—analysis of the pressure distribution. Bubble cavitation is declared when a region of low pressure exists within a region between e.g., 10 and 90% of the blade profiles chord length. The actual inception pressure of bubble cavitation depends on nuclei size distribution in the flow, dissolved gas contents, blade manufacturing tolerance & roughness etc; defining the inception pressure as the vapor pressure plus a margin typically suffices to avoid bubble cavitation. Effectively, the risk of bubble cavitation sets limits on the thickness-to-chord ratio at the lower propeller radii, and sets limits on the curvature of the blade at the higher radii.

The second erosion risk constraint follows from attached or sheet cavitation on the back of the propeller blade. This type of cavitation follows after strong pressure gradients below the inception pressure after which the flow will detach from the blade and a gaseous layer of vapor appears. Attached cavitation may extend (locally) over the full span of blade, and the extent is typically much larger than the region of low pressure predicted by a fully-wetted analysis. Counterintuitively, the effect on efficiency of well-managed attached cavitation for a given propeller is often negligible, while thrust breakdown *may* occur for *some* ships at their highest speeds.

Attached cavitation reacts strongly to loading variations of the blade as it rotates through the ship's wake. The attached cavity volume may collapse quickly into a small volume and its potential energy is transformed into kinetic energy; if the collapse is sufficiently focused in space and repeated with each blade rotation this collapse may become erosive to the blade surface (Bark, Berchiche, and Grekula 2004). If a collapse occurs from the cavity closure towards the blade leading edge, or with the cavity's leading edge collapsing towards the cavity closure—downstream and upstream desinence respectively—then the collapse is nearly always erosive. The dynamic shedding behaviour of the attached cavity is beyond the current capabilities of design tools, nevertheless, we may estimate the risk that shedding occurs following recommendations by (Bark, Berchiche, and Grekula 2004) whereby we analyse the topology of the attached cavity as predicted from PROCAL. A penalty based on cavity

planform of the cavity outline follows. The criterion rewards attached cavities that radially increase in span, connect to the blade tip, and when the blade rotates out of the ship's wake the cavity recedes towards the tip without up- or downstream desinence. Isolated cavities that are formed between the centre or root region of the blade are branded as most unfavourable. The thickness of the cavity is not considered, and when the cavitation locally exceeds the span of the blade (*supercavitation*) no erosion can occur; these properties may be exploited by the optimiser in absence of additional constraints. The use of the cavity outline criterion paired with observations from our testing facilities has proven to be most useful in cavitation management.

The cavitating tip vortex is a major contributor to URN and similar to the attached cavitation, its actual dynamics are most difficult to calculate directly and a subject of ongoing research. The effect of the dynamics of tip vortex on URN is estimated by the *Empirical Tip Vortex* (ETV) model by (Bosschers 2018) further developed within the MARIN Cooperative Research Ships. The model uses the solution from either the fully-wetted or cavitating flow calculation and is coupled to a theoretical model of a cavitating vortex. The model uses empirical factors trained using both model scale and full scale measurements and has been successfully applied to both predict at which conditions inception of the vortex occurs and estimates the contribution of the cavitation vortex to the noise. The model is applied to both face and back side vortices, the latter being the dominant contribution for normal propeller loading. The main driver to the strength of the vortex is the loading at the propeller tip and a high tip loading is generally associated with a good efficiency. Unloading the propeller tip leading to a weaker and often quieter vortex has two effects that require careful attention during the design phase. A tip-unloaded propeller has a reduced effective diameter therefore concentrating the thrust loading to a smaller area, leading to higher energy losses. Also, attached cavitation may be aggravated and isolated from the tip region leading to an increase in erosion risk, a risk that is more often than not mitigated by an increase in blade area ratio leading to further efficiency penalties.

The propeller design is basically a balancing exercise whereby the hindrance effects of cavitation are weighted against the efficiency of the propeller, usually for many operational conditions at once, while being subjected to a host of design constraints. The use of an effective optimisation strategy and an analysis tool with a short turn-around time has made this exercise a manageable problem.

2.5 Estimation of noise levels

Ship underwater radiated noise (URN) is usually quantified in terms of source level (SL) and/or radiated noise level (RNL). The (far-field) sound pressure level (SPL) is the RNL corrected for distance to the source and is directional. The RNL represents the sound level in decibel with reference to 1 μPa m radiated by the source in a lossless medium in the presence of the reflecting sea surface (Lloyd's mirror effect: for deep water with no influence of a sea floor) this effect leads to—on average—attenuation at lower frequencies and amplifying at higher frequencies but is dependent on the position of the source and receiver as well) The SL is closely related to the RNL as (also) a hypothetical point source but in an unbounded ideal fluid without a free surface. For the current study on noise the propeller SL is estimated by various functions (see below) and the RNL is obtained by applying a Lloyd's mirror correction from the ISO 17208-2:2019E norms (eq. 10) (ISO 2019). The background behind this regulation is that the RNL as measured during trials is an average of a recorded signal of three hydrophones at depression angles of 15, 30 and 45 degrees relative to the ship position (perpendicular to the ship course). The average Lloyd's mirror correction for these three signals at those hydrophone locations is specified for an given source depth below the sea surface. The correction is applied here in reverse to obtain RNL from the SL.

The blade-rate contributions of the propeller and its attached cavitation is calculated by PROCAL using the method by (Ffowcs Williams and Hawkings 1969), which is a far-field approach. Therefore, the method is used to compute the sound pressure level at receiver (hydrophone) depression angles at 15, 30 and 45 degrees. Movement of the ship as it sails along these receivers is emulated in ship-fixed coordinates by having copies of these receivers along the track direction within a horizontal beamwise angle of ± 30 degrees resulting in six line arrays. The SPL is subsequently corrected to a mean RNL of each line array, summed for each blade-rate frequency and that mean added to the total.

Several semi-empirical sound prediction models were coupled to our workflow to calculate their contributions to the propeller's SL, namely the contribution of the sheet and tip vortex cavitation sound sources, the blade rate contributions and machinery noise, see Figure 2-7 presented in power spectrum in decidecade bands (or, one-third octave bands, base 10), see ISO 18405-2:2017E norms(ISO 2017).

The SL of the attached cavitation can be estimated using the relation by Brown (Brown 1976) as applied in SDC9/INF.11. Within the EU NAVAIS project, the correlation between the model of Brown and attached cavitation on the face of the propeller blade did not match a number of measurements performed at MARIN and a new model was developed (Lafeber et al., 2022,). These models estimates the peak frequency in the spectrum based on the cavitation number and the maximum cavitating (non-wetted) area of a single blade, using a plateau for the spectrum below this peak frequency followed by a linear decay. These sheet cavitation sound models do not take the dynamics of the cavity itself into account. As the NAVAIS model has been trained on a large set of propellers designed for efficiency, acceptable hull-force fluctuations and low erosion risk following model tests, we argue that *if* a propeller meets our demands low erosion risk as per our cavity outline criteria, *then* the NAVAIS model is a good empirical estimator for the SL of the attached cavity.

The SL for the tip vortex is estimated by the *Empirical Tip Vortex* (ETV (Bosschers 2018)). The model is applied to both face and back side vortices. The empirical model is tuned on the back side vortex that is usually the dominant contribution to the overall SL for normal propeller loading. A spectral shape is prescribed of a low-frequency hump and a high-frequency linear slope. Both the noise levels as well as the hump centre frequency depend on the tip loading and cavitation number following a detailed analysis of a specific propeller operating in the ship's wake. As such it responds to the changes proposed by the optimiser and when the strength of the vortex decreases both the overall noise levels reduce and the centre frequency of the hump increases, changing the overall spectral shape.

The machinery noise is estimated using the respective components from the recently developed semi-empirical PIANO model (Lloyd, Daniel, et al. 2024), which makes a distinction between the noise from

cavitation and from machinery. The purpose of the PIANO model is to estimate the SL at a fleet level and relies on its own educated guesses for the model input parameters, which include several ship and propeller properties. Here we have access to most information of the ship such as the hull shape and flow simulations, model test results and the propeller geometry. While the main engine of this particular ship is known, the auxiliary engines are not and they were estimated from comparable ships; their contribution had no impact on the results.

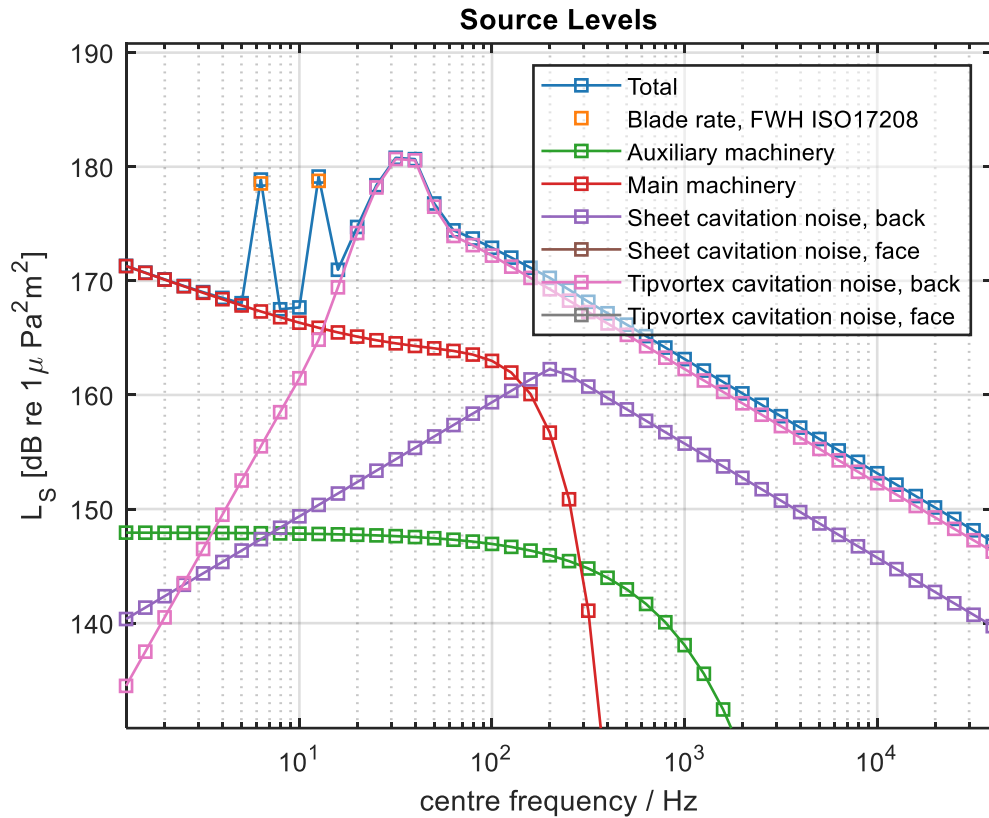


Figure 2-7 - Typical results of an estimated total propeller source level and its constituents as a power spectrum (decade bandwidth levels). Some contributions (here: face-side sheet and tip vortex) do not appear.

3 TRADE-OFF BETWEEN URN AND GHG

The previous section provided an introduction of the propeller geometry description, the optimisation procedure, the constraints applied to obtain industry standard propeller designs and how the source level distribution was estimated using our propeller analysis tool. This section discusses the outcome of the optimisation procedure for its two goals: the propeller power required to obtain a ship speed of 19.75 knots and the overall propeller source level within a frequency range of 1 Hz to 50 kHz. These results are then analysed for the trade-off study of URN vs GHG when sailing through a zone with noise restrictions.

Note: the engine selected for the actual vessel has a maximum continuous rating of 26,150 kW at 76.0 rpm, at which the ship is expected in service conditions to obtain a speed of 19.75 knots. This exact point is taken as a reference point to design the propellers' effective pitch. Later on in this study, in order to be consistent with SDC9/INF.11, it is assumed that sufficient engine power is available for the ship to attain a speed of 21.5 knots with the required power following from the model test results.

3.1 Results of the propeller design study

The optimisation progression is plotted in Figure 3-1, with a close-up of the Pareto front in Figure 3-2. The colour scale from blue to red indicates the progression over the generations, a cross denotes an infeasible design. The process is as typically observed for propeller optimisation with the earliest generations all infeasible, not particularly efficient and showing very high overall source levels. The optimiser first focusses on satisfying constraints and once the early designs are found the solution usually shifts towards the (final) Pareto front. While new designs are being found as late as generation 100, the results are not expected to improve appreciably and are well suited for our follow-up analysis.

From the close-up Figure 3-2 we find a well-defined trade-off between overall source level and efficiency. The efficiency varies between 67.0% to 73.2% and the overall SL ranges from 181.9 dB to 190.8 dB; there is a clear trade-off: reducing noise demands deduced cavitation extents and these restrictions come at a cost. The overall slope of the Pareto-front is shallow below a propeller efficiency of 70% where the noise levels are hovering at 182.5 dB; if we take the 70% efficiency as reference, a relative increase of 4.5% power is needed to obtain 0.6 dB only, in the region of diminishing returns. Closer inspection—not presented—revealed that the most quiet propellers do not have sheet cavitation and the only appreciable noise contribution is from the tip vortex at about 140 dB in the 100-200 Hz region. For these propellers the contribution of the machinery is dominating and the propellers are insignificant in terms of overall source level. Above a 72% efficiency the cavitation noise is the dominant noise source increasing by as much as 5 dB to arrive at 73%. These results suggest, assuming that most propellers are selected for their fuel economy, that relatively small sacrifices in propeller efficiency may already yield large gains in noise reduction.

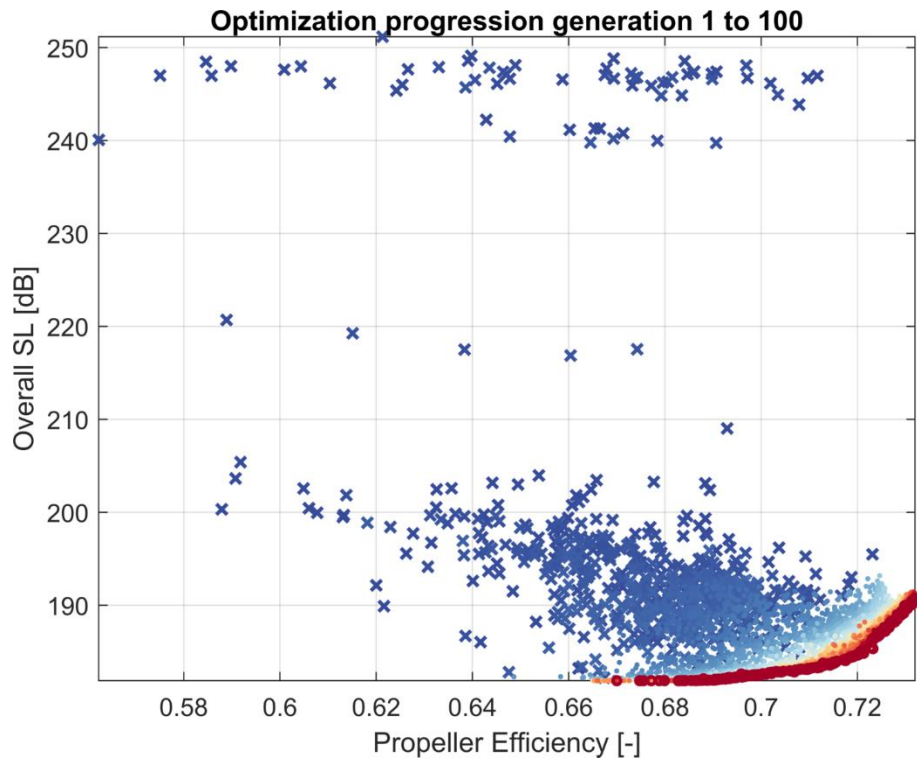


Figure 3-1 - Full optimisation progression.

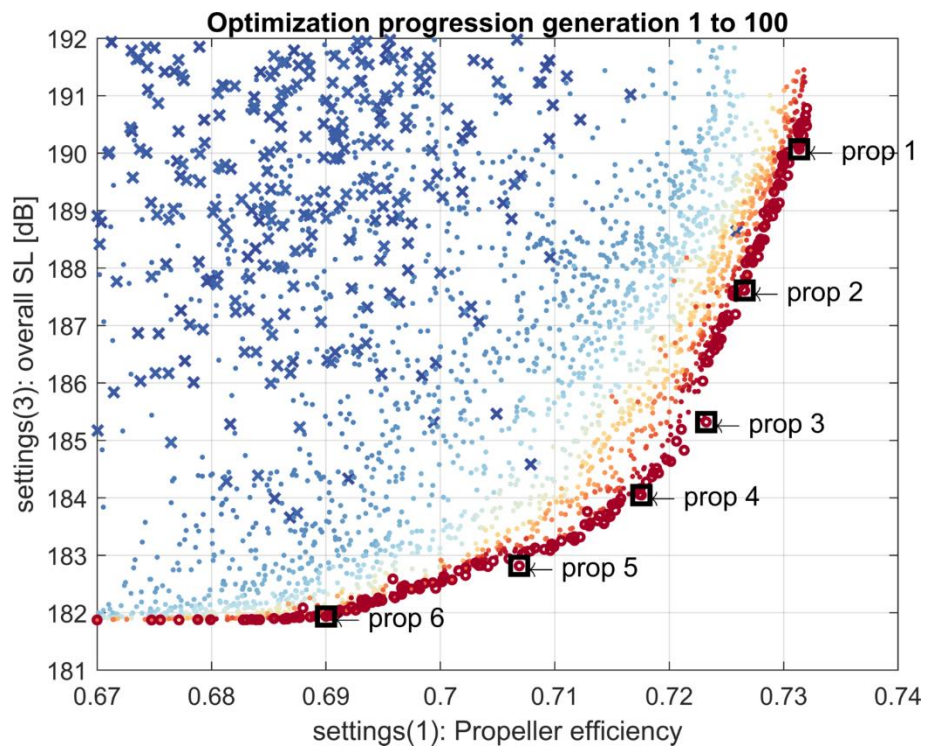


Figure 3-2 - Optimisation progression, Pareto-front close-up, plus 6 propellers selected for further study.

In this section we revisit the document SDC9/INF.11 and perform a similar study using the collection of propeller designs from our previous section. From this collection of Pareto-optimal designs, six designs are isolated for further analysis, see Figure 3-2, Figure 3-3. These individuals were selected to capture the Pareto-front, with three propellers on the right flank where the SL reduces sharply as a function of efficiency, and three propellers at the left side whereby the engine contribution becomes dominant. From the renderings it follows that the blade length in the tip region increases from propeller 1 to propeller 6.

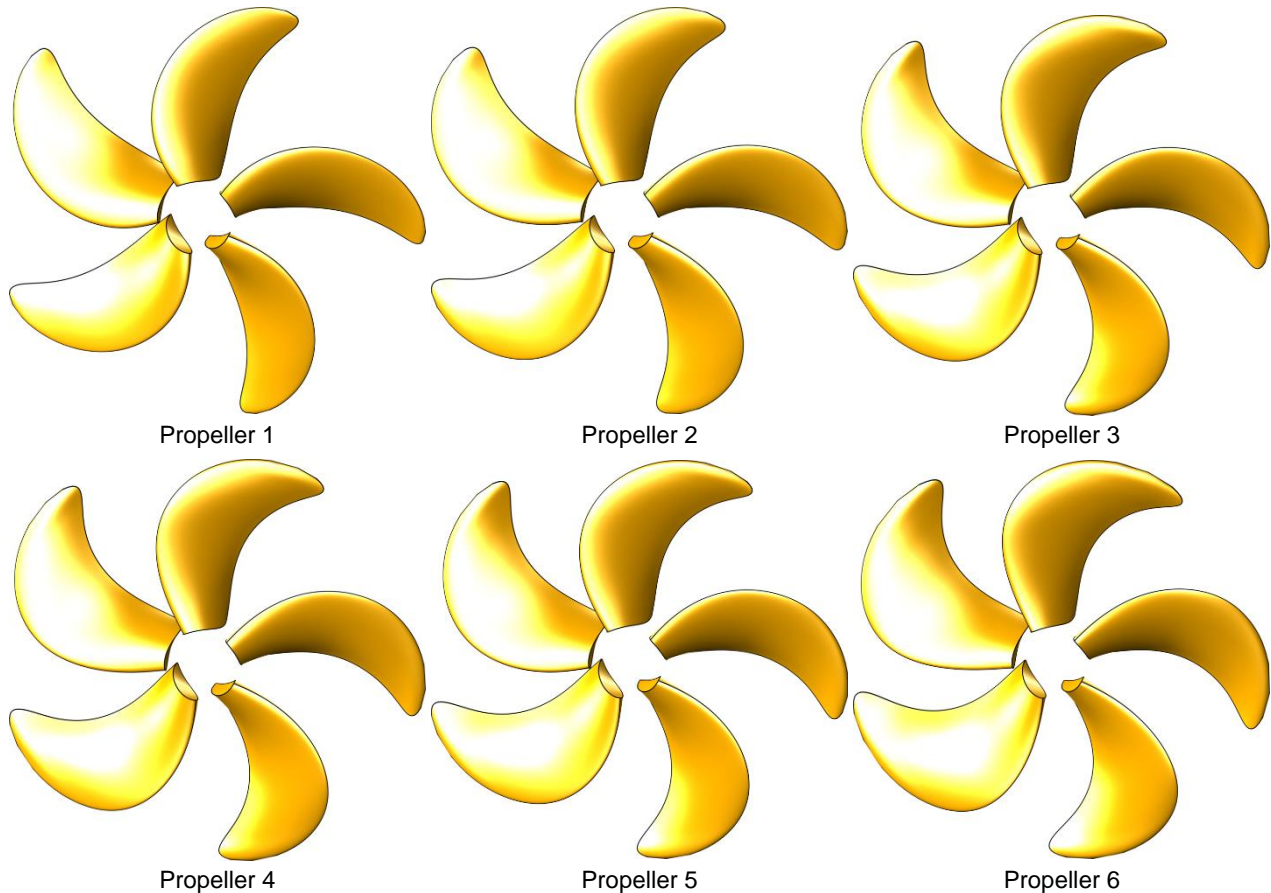


Figure 3-3 - 3D renderings of propellers 1 to 6.

Several properties of these propellers are given in Table 3-1. Along the Pareto front the Blade Area Ratio (BAR) increases from 49.1 to 61.7%; a narrower range than in SDC9/INF.11 where the BAR was varied between 50 and 100%; from the optimisation it follows there is no need for larger blade area ratios to significantly reduce the noise levels.

From an efficiency point of view only, an optimal diameter can be estimated for the propeller using available performance data of reference propeller series; for the current ship the optimal diameter is just below the maximum for this vessel (9.6m). The general effects of the selection of propeller diameter remain; increasing the diameter (usually) leads to an improvement of efficiency, but also reduces the distance between the hull and propeller affecting propeller-induced hull pressure fluctuations—onboard noise and vibrations—and increases the tip speed possibly increasing noise. These more nuanced trade-offs are difficult to predict without a detailed analyses and were therefore left to the optimisation process. While the diameter was free to vary, it reduces only slightly from 9.6 m to 9.5 m over the Pareto front.

The last four columns in Table 3-1 report the RNL at a ship speed of 18 knots, the first three the power spectral values in dB of the maximum encountered, the value from the 63 Hz and 125 Hz bands, and finally the overall levels integrated over the entire frequency range from 1 Hz to 50 kHz. These values are also plotted in Figure 3-4. For these six propellers the overall, maximum and levels in the 125Hz bandwidth show the same trend. The trend for the 63Hz band deviates and is discussed below.

Table 3-1 - Selected properties of propellers 1 to 6 at a service speed of 18 knots.

prop	BAR	D	efficiency	max(L)	$f_{\max L}$	$L_{RN,63}$	$L_{RN,125}$	L_{OA}
	[%]	[m]	[%]	[dB]	[Hz]	[dB]	[dB]	[dB]
1	49.1	9.60	73.1	178.7	40	175.2	173.9	185.9
2	51.6	9.59	72.7	175.7	40	172.8	171.4	183.2
3	54.4	9.59	72.3	174.5	50	172.4	170.0	181.5
4	55.7	9.59	71.8	173.5	63	173.5	169.1	180.4
5	57.1	9.53	70.7	171.4	80	170.1	167.5	178.1
6	61.7	9.47	69.0	166.6	80	166.1	165.4	175.0

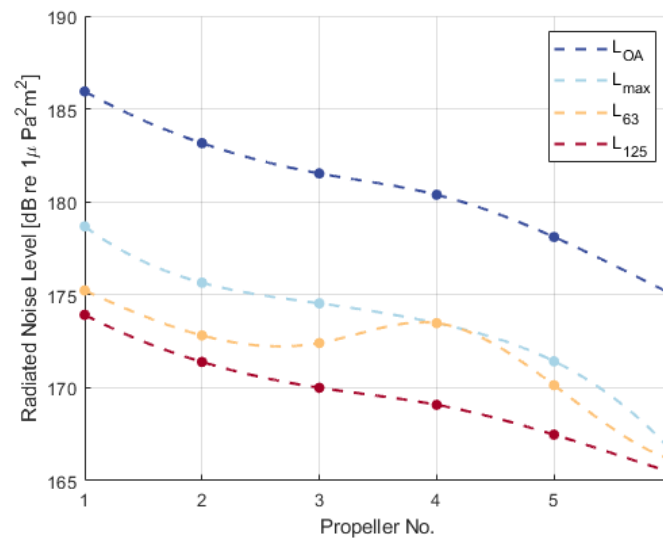


Figure 3-4 - Various RNL metrics along the Pareto Front, ship speed 18 knots.

3.2 Effect of slow steaming and propeller design

The operational speed of the ship lies at 18 knots with a maximum ship speed at around 19.75 kts; the propeller cavitation is designed to be well managed upto the maximum ship speed. The estimated RNL at the ship design speed of 19.75 knots is presented in Figure 3-5 including the DNV 2018 SILENT-E (Environmental) class transit and quiet notations (vessels with this class are able to document noise performance to authorities). For the most efficient propeller (prop 1), the effect of the tip vortex noise is dominant, with the characteristic hump around 30-40 Hz. A close-up is given in Figure 3-6; the centre frequency of 63 and 125 Hz bandwidth as specified in the Good Environmental Status assessment of the European Union's Marine Strategy Framework Directive (EU 2017) accentuated.

Note— while the overall noise levels show considerable differences— that the model predicts identical RNL levels for propellers 3 to 5 in the 63 Hz band. Since from propeller 1 to propeller 6 the noise levels decrease by virtue of a smaller contribution of the tip vortex noise, the hump in the spectrum decreases, but also shifts towards higher frequencies, into the 63 Hz band. This effect is not observed for the 125 Hz band. These results do suggest that a focus on the reduction of RNL within a single decade band may not have sufficient resolution per se to capture the effects of a change of a propeller design.

In Figure 3-7 the ship noise as a function of ship speed is plotted, with the contributions of the machinery, cavitating tip vortex and attached cavity plotted as well.

1. The contributions of the attached cavity are visible in the lower-right corner of the figure and are observed to increase rapidly with the onset of attached cavitation on the blades. However, even near the maximum ship speed for the least quiet propeller the model does not contribute appreciable to the overall noise levels. Note that we used the NAVAIS model, and not the model by Brown. When using the latter (not presented), the contribution at the maximum ship speed is quite similar.
2. The most quiet propeller follows the machinery noise contribution, confirming that this propeller has its cavitation reduced by such a degree that it is no longer contributing. Further reductions in noise levels cannot be obtained without addressing the machinery noise.
3. For most other propellers it is observed that the tip vortex model is the main driver of the ship noise profile, more so at the higher ship speeds.

Clearly, by following the approach as in the PIANO model of considering the machinery and propeller noise separately we find different trends in the noise profile for a single vessel as a function of propeller design only, compared to only using the Brown model as was done in SDC9/INF.11. In Figure 3-8 the overall ship noise levels are repeated including two sketches indicating a power-law dependence of $RNL \propto 10 \log_{10} V_S^{pow}$ for exponents of $pow = 2.5, 6$; the latter value of 6 is often used by models to estimate ship noise when only limited data is available such as a Jomopans-Echo model (A. MacGillivray and De Jong 2021); this aspect is discussed in detail in part two of this study in report 77002-3-RD. It is observed that the quiet propeller design that is dominated by machinery noise is close to a $RNL \propto \log_{10} V_S^{2.5}$ relation, and, for the most efficient propeller it is observed that the noise levels do not follow a unique $RNL \propto \log_{10} V_S^{pow}$ relation for the whole speed range but in fact increase more strongly as a function of ship speed. This may mean that when more generic models are used that the effects of slow steaming on noise for quiet propellers will be overestimated and that the effects of slow steaming on noise for highly efficient propellers will be underestimated.

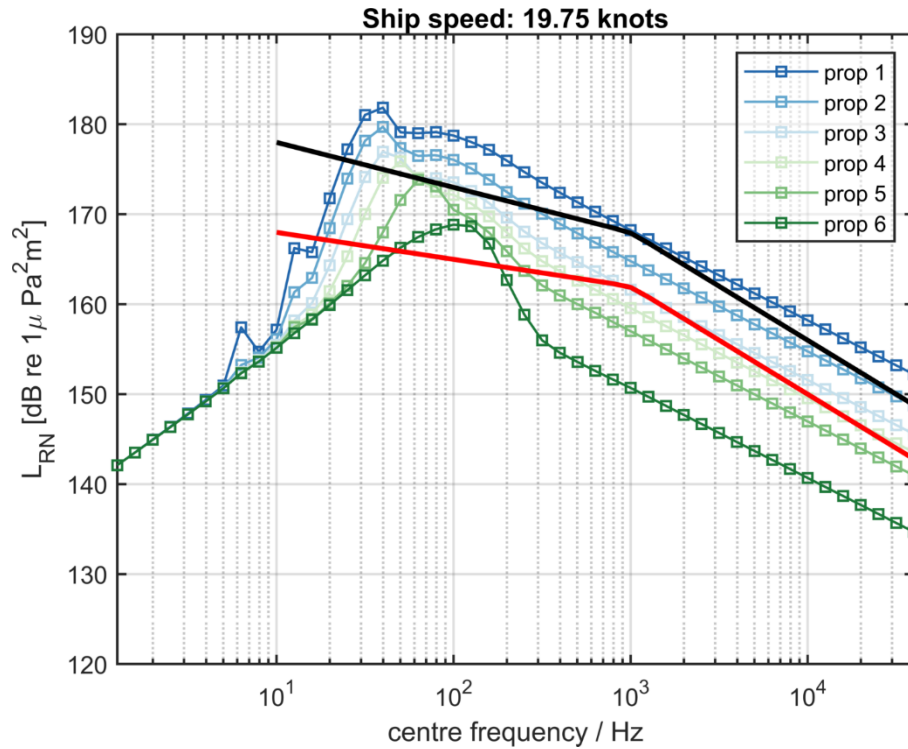


Figure 3-5 - RNL for the six propellers at the ship design speed. The black and red line denote the DNV SILENT-E transit and quiet class notations, respectively.

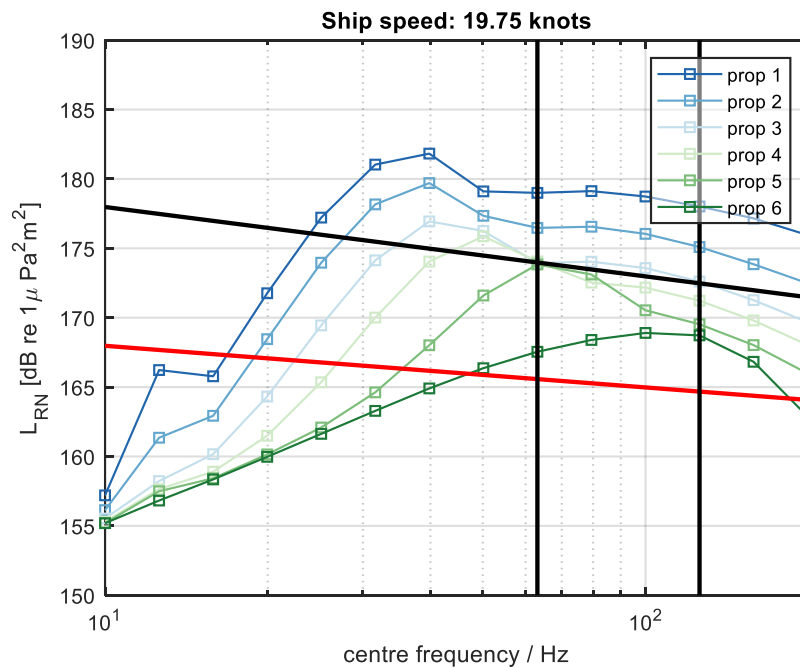


Figure 3-6 - Close-up of Figure 3-5, 63 and 125 Hz centre frequency location indicated by vertical black lines.

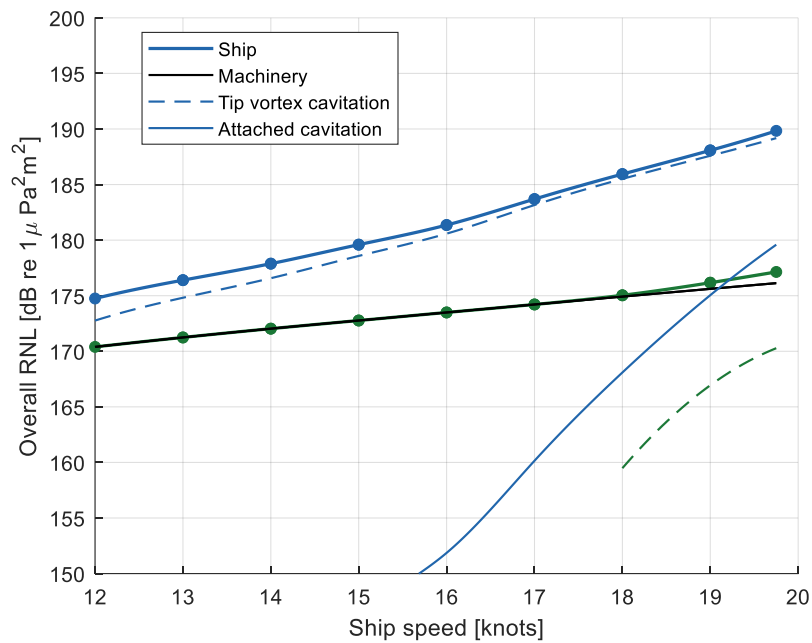


Figure 3-7 - Overall RNL as a function of ship speed, separately showing the contribution of the machinery, tip vortex and attached cavitation, for propellers 1 (blue) and 6 (green).

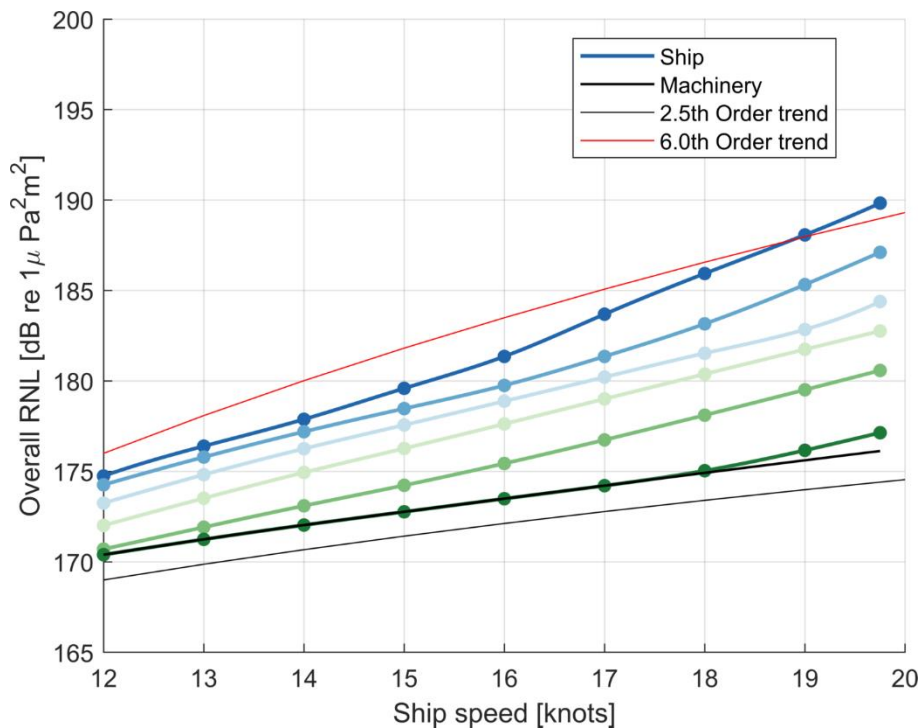


Figure 3-8 - As Figure 3-6, showing overall Ship noise only and two assisting lines $RNL \propto \log_{10} V_S^{pow}$ for exponents 2.5 and 6.

3.3 Revisiting SDC9/INF.11

Following SDC9/INF.11 a scenario is analysed whereby a ship needs to reduce speed to meet certain noise limits over a part of its journey. We assume the ship will sail through a region—the quiet zone—where restrictions in allowable radiated noise levels apply: the ship will slow down in order to not exceed set limits. Outside these quiet zone the ship will sail faster to make up for the lost time as a delay in arrival time is not permitted. The ratio of the length of the quiet zone compared to the total track is referred to as the track ratio. In Figure 3-9 an example is given for the ship with a service speed on 18 knots sailing through regions whereby a 14.5 knots speed is given with a varying track ratio, showing the required speed increase outside the quiet zone, as a function of the voyage duration. When the track ratio is 40%, the time spent in that quiet region is 50% of the voyage duration.

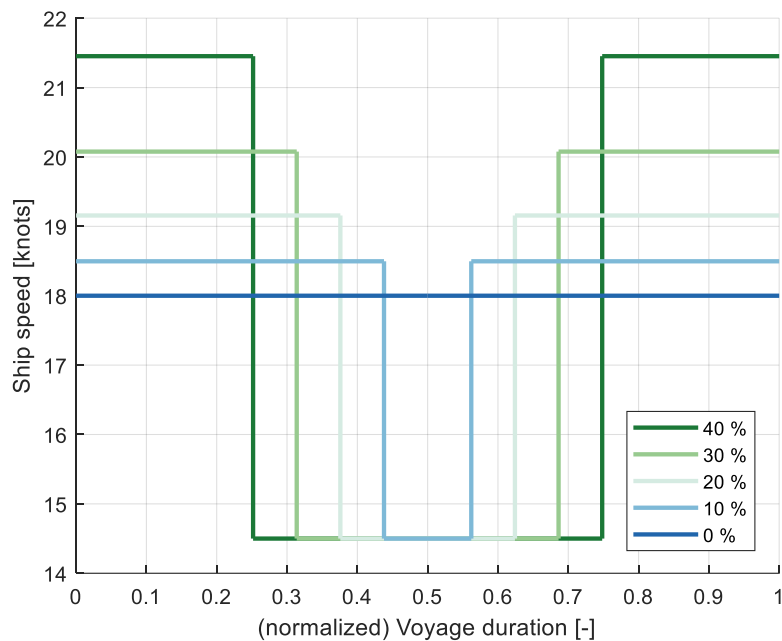


Figure 3-9 - Ship speed as a function of voyage duration for various track ratios, assuming the ship sails 14.5 knots in the quiet zone.

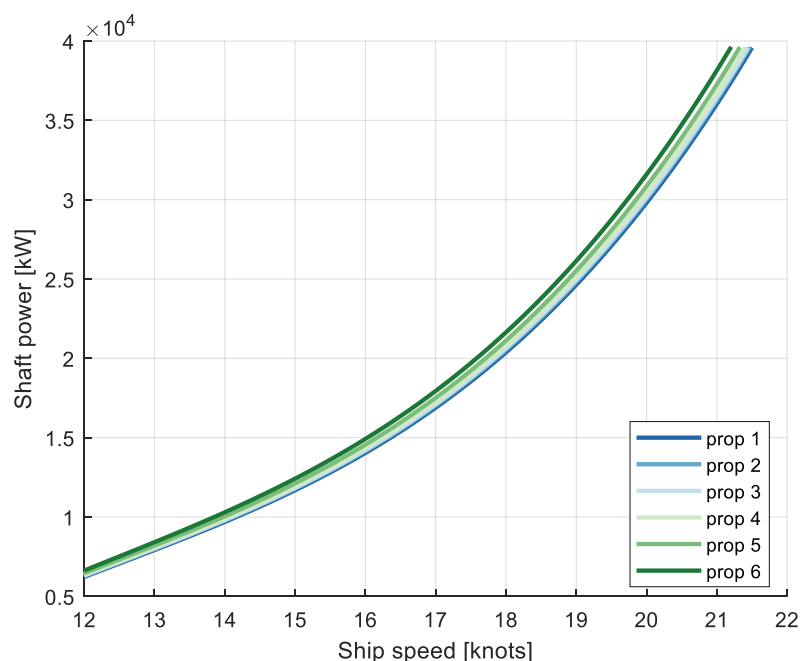


Figure 3-10 - Computed speed-power relation for all six propeller designs using model test results.

While our example vessel has been designed for a (service) speed of about 20 knots, we will assume the vessel is able reach a top speed of 21.5 knots in line with SDC9/INF.11. From the model tests performed it follows that this change in maximum speed requires an engine power increase of 36%. The effect of the reduced efficiency on the maximum speed has been taken into account and the least efficient propeller has the maximum speed reduced by about 0.35 knots—given the same installed engine power—and Figure 3-10 presents the power-speed relationship of the vessel for all propellers. The effect of this larger engine on noise was not taken into account; the 36% increase in power results in a machinery noise increase of only 0.8 dB and will not change the conclusions.

What constitutes a realistic noise restriction regulation is a matter of considerable debate. Focusing on a single decidecade frequency band *may* obscure the effect of a new propeller design. In the ECHO & Quiet Sound voluntary slowdown programmes (Quiet Sound programme 2024; Vancouver Fraser Port Authority 2023) a speed reduction at 14.5 knots was proposed. For this study we have taken the DNV SILENT-E Class; Transit notation offset by -3 dB. By applying this limit the ship with the reference propeller 1 obtains a quiet speed of 14.3 knots, close to the recommended 14.5 knots for container ships. Next, we assume that for each propeller variant, the vessel is certified to have a low-noise speed—the quiet speed—where the ship will not exceed a given RNL level within any decidecade frequency band; the quieter the propeller the higher the quiet speed. In Figure 3-11, the quiet speed for each propeller is plotted versus the relative efficiency. For the most efficient propeller the quiet speed is about 14.3 knots while for the most quiet propeller the quiet speed is well over its service speed of 18 knots and requires no slowdown in the quiet zone; in fact, the quiet speed lies around 20 knots. From Figure 3-11 it also follows that the relationship between the quiet speed and efficiency is found to be nearly linear. For each 1% drop in efficiency the quiet speed increases by 1 knot.

It is emphasised that the limit used here was obtained to arrive at the 14.5 knots voluntary slowdown speed for the most efficient propeller and is intended to be used to gauge the effect of propeller design on URN, and that, given the uncertainties in the sound models used in this study, is not proposed as an actual operational limit.

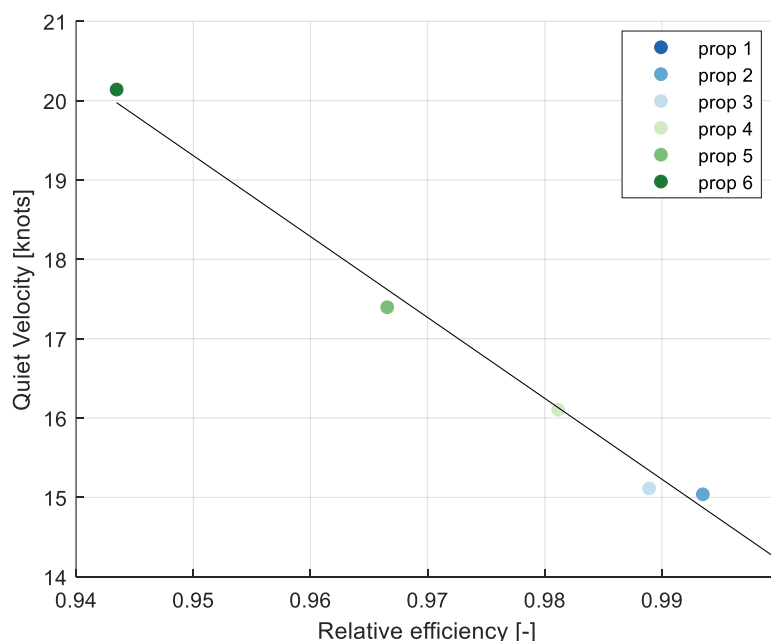


Figure 3-11 - Margin against exceeding assumed RNL limits in dB in the quiet zone as a function of ship speed and efficiency relative to the most efficient propeller.

As the track ratio increases so does the time lost to meet the arrival time; the track left to make up for lost time becomes progressively smaller compounding further to the need to increase speed. The required speed is given in Figure 3-12; once the ship speed reaches its maximum the ship can no longer arrive on time.

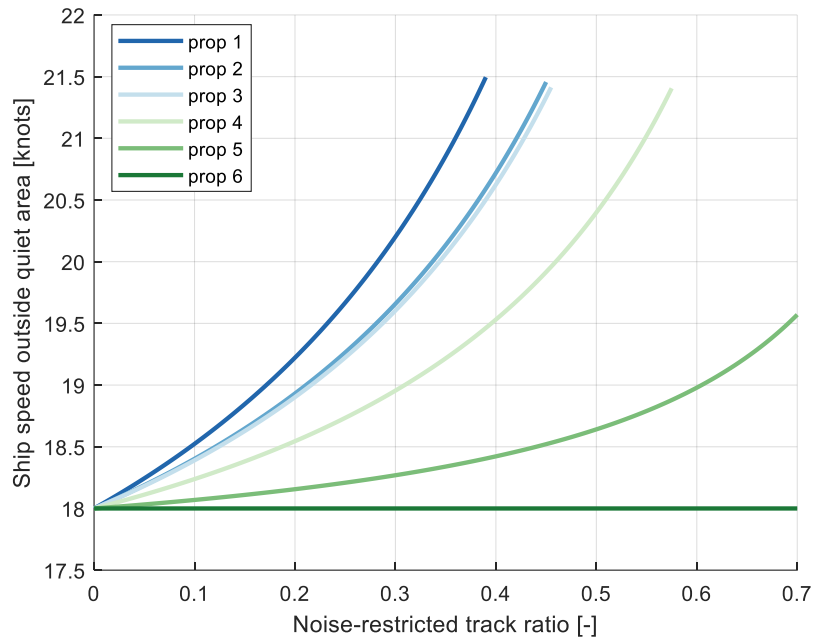


Figure 3-12 - Increased ship speed outside quiet zone as a function of the track ratio.

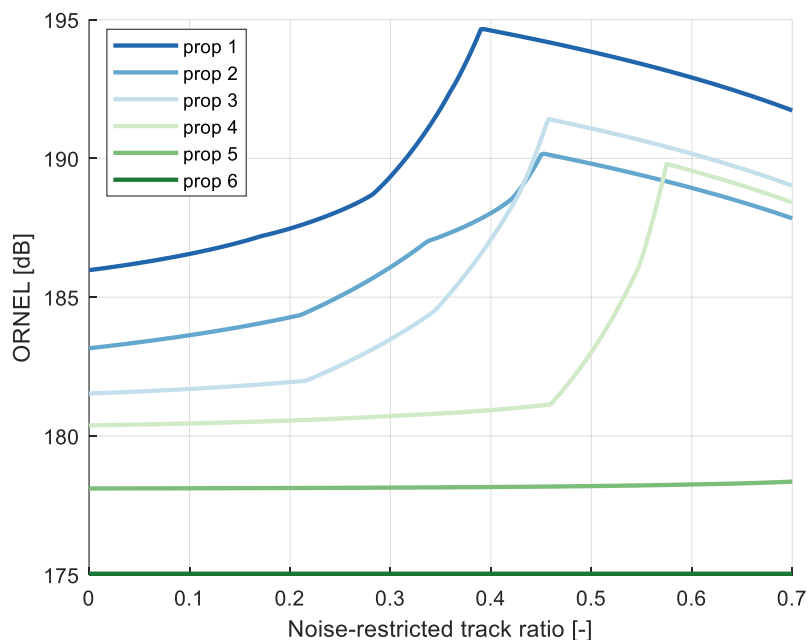


Figure 3-13 - ORNEL vs track ratio, propellers 1 to 6.

In Report 77002-3-RD the so-called Overall Radiated Noise Exposure Level is introduced

$$ORNEL \equiv 10 \log_{10} \sum_{f=f_1}^{f_2} \sum_{i=1}^N 10^{L_{RN,i}(f)/10} \Delta t_i \quad (1)$$

or more simply put, the sum of time-weighted RNL contributions over all decade frequency bands, with Δt_i normalised by the total travel time of the ship at the normal service speed (i.e., 0% noise-restricted track ratio). Here we have at most two conditions at the quiet and overspeed conditions. This quantity might give a better indication of the overall hindrance the vessel as it includes the increases in sound production outside the quiet region, see Figure 3-13. From this figure it follows that the overall exposure at no point reduces below the values of operating sailing at the design speed of 18 knots (with no quiet region, or track ratio equal to zero). The more quiet propellers nearly always have a lower overall ORNEL value.

Recall that the propellers were initially designed for a maximum speed up to 19.75 knots and no constraints were given for ship speed of 21.5 knots that was later assumed in this study; this is apparent in the ORNEL behaviour of all propellers that increases sharply about 20 knots, yielding a steep increase in the ORNEL as well. This steep increase may not be fully representative if the propellers were designed taking the 21.5 knots condition into account, although overall behaviour is not expected to change.

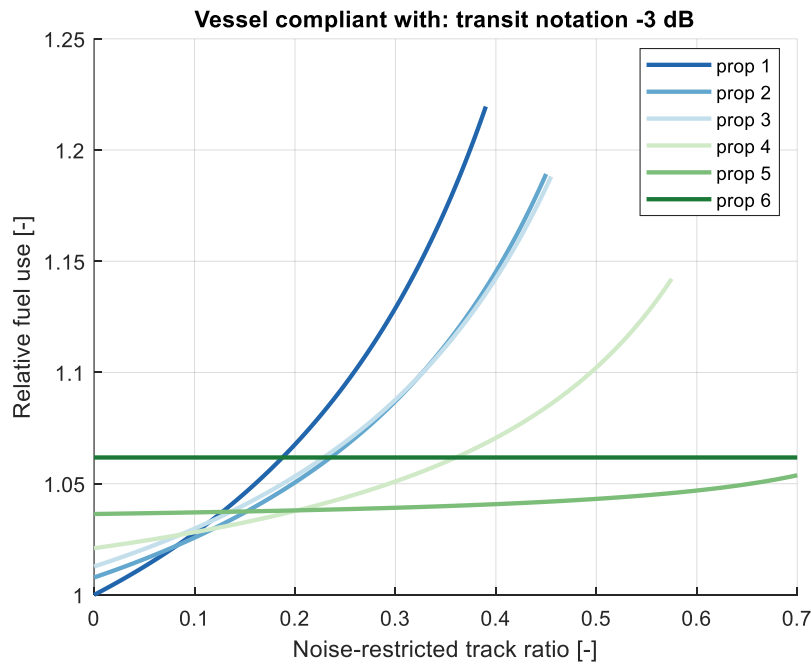


Figure 3-14 - Relative fuel use as a function of track ratio, all propellers.

The result for the change in fuel use for all propellers is plotted in Figure 3-14 with reference to the fuel use of propeller 1 at a zero track ratio. While less time is spent at higher speeds as the track ratio increases, the exponential relation between ship speed and required power results in a net increase of required energy over the voyage, or, fuel use compared to the baseline of sailing at 18 knots service speed and zero track ratio (i.e., no quiet zone).

The most efficient propeller (prop 1) shows the steepest increase in fuel use with the increase in track ratio as this propeller incurs the largest speed reduction to 14.3 knots and the largest increase in operational speeds outside the quiet zone. When the track ratio is 0.40 the maximum speed is exceeded and the ship can no longer arrive on time.

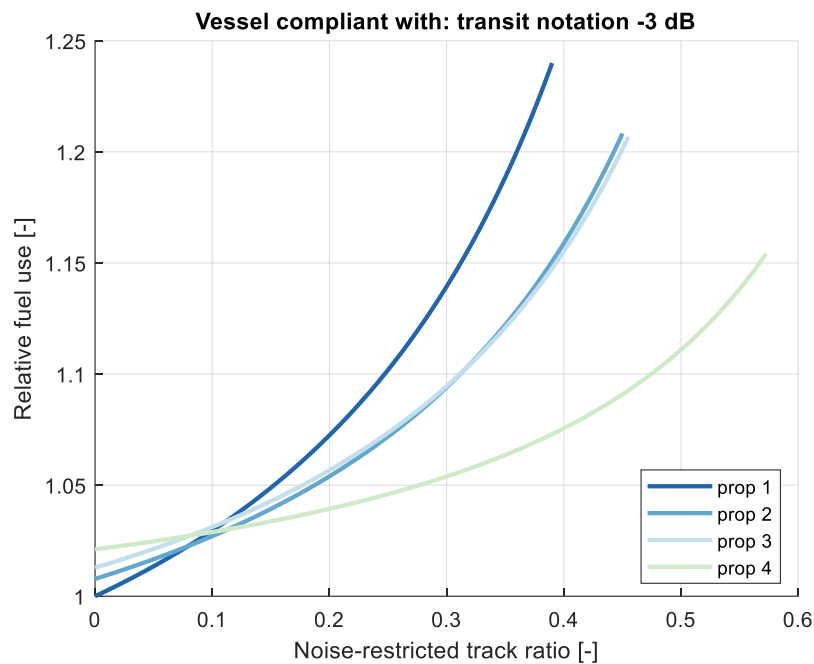


Figure 3-15 - Relative fuel use as a function of track ratio, propellers 1-4.

The comparison between propellers (1) and (2,3) shows that for a track ratio exceeding about 10% the net fuel use of propellers (2,3) is lower than for propeller (1) at the cost of 1% loss in efficiency.

It was earlier concluded that in terms of overall noise levels a decrease is found from propeller (1) to (4) commensurate with the efficiency loss. Counterintuitively perhaps, in Figure 3-15 it is observed that for propeller (4) its 2% efficiency loss outperforms propellers (2,3) in terms of overall fuel use at the same track ratio of 10%. The balance between noise and net fuel use is such that more substantial losses are called for to obtain low noise designs and the more modest changes to the propeller designs are not effective measures in our scenario.

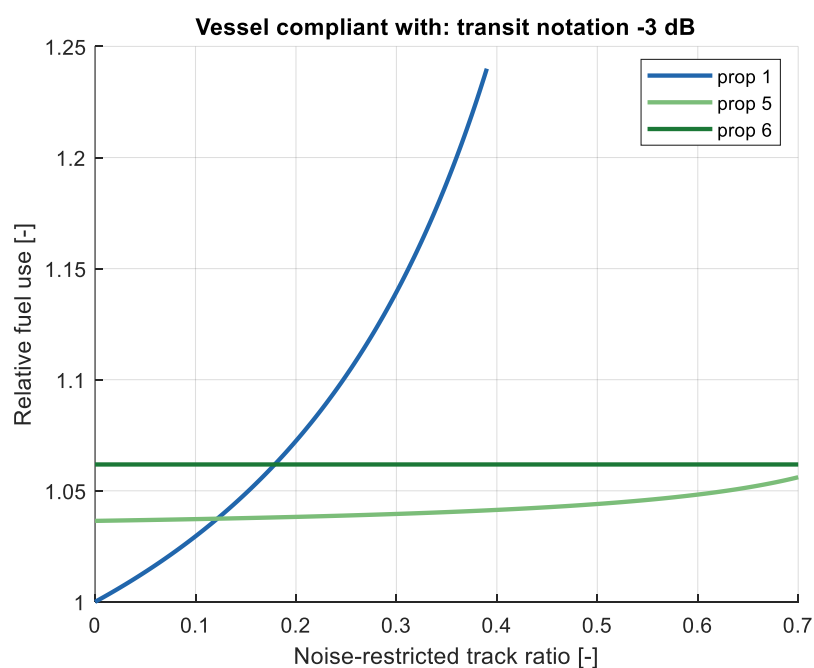


Figure 3-16 - Relative fuel use as a function of track ratio, propellers 1, 5, 6.

For the most quiet propeller (6) no speed reduction is required and compared to propeller 1 at a track ratio of about 18% this design has a total lower fuel use. However, when comparing the most quiet propeller to its nearest neighbour it is observed that propeller (5) has a lower total fuel use for a track ratio around 75%. Propeller (5) is also more fuel efficient than propeller (1) at a track ratio just under 15%. The quiet speed of propeller (6) is estimated at 20 knots and with an efficiency loss of about 1% per knot of the quiet speed, this propeller overshoots the noise requirement and is 2% too low in efficiency at a total decrease of 6%.

If we were to select a propeller for its lowest overall fuel consumption at a given track ratio it is recommended that:

- For a track ratio below 10% select the most efficient propeller (1).
- For a track ratio between 10 and 20%, select propeller (4), which is 2% less efficient.
- For a track ratio over 20%, select propeller (5), which is 4% less efficient.
- Do not select the propeller that is 6% less efficient and that meets the noise limitations at ship speeds exceeding its required service speed.

4 CONCLUSIONS AND RECOMMENDATIONS

Anthropogenic underwater noise has increased significantly since the industrial revolution and is negatively affecting the marine soundscape (Duarte et al. 2021). Shipping noise is recognised the most ubiquitous and pervasive source with effects on marine life ranging from changes in behavioural response, masking of communication and echolocation, and stress (Erbe et al. 2019). This reports focusses a technical solution to reduce shipping by means of propellers design.

In November 2022 Japan submitted their document SDC9/INF.11 to the IMO reporting a study on the effect of propeller design with varying noise levels and efficiencies on overall fuel use; a container vessel was assumed to reduce speed in regions where noise restrictions apply—the quiet zone—followed by an increase in speed so that the arrival time remained unchanged. In the study by Japan the noise was estimated using Brown’s model for sheet cavitation only and the extent to which the propeller geometry was varied was unknown. Here, the Japanese study was repeated for a container ship recently tested at MARIN using the propeller optimisation tools to extensively explore the design space, and, using the latest versions of sound source level estimation functions for various types of cavitation and machinery noise.

In the current study the optimisation procedure was able to find a range of propeller designs whereby a clear trade-off between noise and efficiency was found; the least efficient propeller was free of attached cavitation at the service speed with overall ship noise was dominated by the machinery noise. The most efficient propeller’s noise was dominated by the cavitating tip vortex. A noise limitation based on class society quiet notations was introduced such that the most efficient propeller is compliant at a ship speed of 14.5 kts, following the recommended voluntary slowdown speed from the ECHO program. For each propeller design the quiet speed at which this limitation is not exceeded was estimated. The propeller design study showed that the ship with the most efficient propeller incurs a slowdown to 14.3 knots while the most quiet propeller meets the noise limit even above the ship service speed of 18 knots.

From a comparison of several propeller designs it follows that depending on the track ratio—the ratio of the lengths of the quiet zone whereby the noise limitations may not be exceeded and the total track length—an optimal efficiency loss between 2 and 4% is found whereby the net fuel use is lower than the propeller with the highest efficiency. For these propellers it was observed that

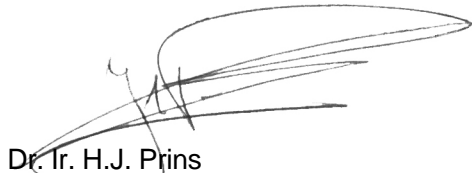
- Propeller designs with a 1% efficiency loss have a higher net fuel consumption than designs with a 2% efficiency loss above a track ratio of 10%.
- The quietest propeller, with an estimated 6% efficiency loss—and no attached cavitation—overshoots its mark by meeting the assumed restrictions of the quiet zone at a ship speed exceeding its operation service speed. As a result, it has a higher overall fuel consumption than a propeller with a 4% efficiency loss, for a track ratio below 75%.
- The propeller with a 4% efficiency loss has the lowest overall fuel consumption above a track ratio of 20% compared the propellers with a higher efficiency.

It is concluded that the results of the IMO SDC9/INF.11 are confirmed from a qualitative point of view, but the present detailed propeller design study shows that if a noise limit applies on a track a more quieter propeller design is more favourable. The following key differences are observed

- The contribution of noise estimation models, in other that for sheet cavitation, in particular those of tip vortex and machinery noise, had an important influence of the propeller designs. The blade-area ratio required to manage cavitation varied only slightly, from 50 to 60%, while SDC9/INF.11 used a variation on blade-area ratio of 50 to 100%. A larger blade area ratio typically implies a larger loss in efficiency, a larger propeller mass and higher manufacturing costs. The upper limit of the efficiency loss of 8% reported in SDC9/INF.11 is twice the required efficiency loss reported here.
- SDC9/INF.11 (19) concluded that when the quiet zone is small it is advantageous to select the most efficient propeller. When the track ratio—the ratio of the lengths of the quiet zone and the total track length—is more than 25%, then a more silent propeller design is more fuel efficient. In the current study was found that a more silent propeller is more fuel efficient at a track ratio as small as 10%.

The above conclusions do not generally apply to all ships or even ships of the same type. For this modern container vessel the optimisation procedure was able to obtain a family of propeller designs tailor-made for the specific hull form, (to be) installed engine and operational profile. Propeller designs were found that were not even contributing to the overall noise levels of the ship, i.e., whereby the estimated engine noise was the dominant contribution; other technical mitigation measures would be required to reduce the noise further. For slower, fuller ships with a less favourable inflow towards the propeller—tankers, bulk carriers, particularly in ballast conditions—such nearly-cavitation free designs may either be not possible at all or at a much larger efficiency penalty, skewing the relation between overall sound levels and ship speed. Studies akin to the current work are recommended for other ship categories.

Wageningen, March 2025
MARITIME RESEARCH INSTITUTE NETHERLANDS



Dr. Ir. H.J. Prins
Manager Research & Development

REFERENCES

- Bark, G, N Berchiche, and M Grekula. 2004. "Application of Principles for Observation and Analysis of Eroding Cavitation - The EROCAV Observation Handbook." Technical report. Chalmers University of Technology.
- Bosschers, J. 2018. "A Semi-Empirical Prediction Method for Broadband Hull-Pressure Fluctuations and Underwater Radiated Noise by Propeller Tip Vortex Cavitation †." *Journal of Marine Science and Engineering* 6 (2): 49. <https://doi.org/10.3390/jmse6020049>.
- Brown, N. A. 1976. "Cavitation Noise Problems and Solutions." In *Proceedings of International Symposium on Shipboard Acoustics*. 6th-10th September, Noordwijkerhout, The Netherlands.
- Deb, K. 2000. "A Fast and Elitist Multiobjective Genetic Algorithm." *Computer Methods in Applied Mechanics and Engineering* 186 (2–4): 311–38.
- Deb, K, A Pratap, S Agarwal, and T Meyariyan. 2002. "A Fast and Elitist Multiobjective Genetic Algorithm: NSGA-II." *IEEE Transactions on Evolutionary Computation* 6 (2).
- Duarte, Carlos M., Lucille Chapuis, Shaun P. Collin, Daniel P. Costa, Reny P. Devassy, Victor M. Eguiluz, Christine Erbe, et al. 2021. "The Soundscape of the Anthropocene Ocean." *Science* 371 (6529): eaba4658. <https://doi.org/10.1126/science.aba4658>.
- Erbe, Christine, Sarah A. Marley, Renée P. Schoeman, Joshua N. Smith, Leah E. Trigg, and Clare Beth Embling. 2019. "The Effects of Ship Noise on Marine Mammals—A Review." *Frontiers in Marine Science* 6 (October):606. <https://doi.org/10.3389/fmars.2019.00606>.
- EU. 2017. "Commission Decision (EU) 2017/848 of 17 May 2017 Laying down Criteria and Methodological Standards on Good Environmental Status of Marine Waters and Specifications and Standardised Methods for Monitoring and Assessment, and Repealing Decision 2010/477/EU." *Official Journal of the European Union* 125 (May):43–74.
- Ffowcs Williams, J. E., and D. L. Hawkings. 1969. "Sound Generation by Turbulence and Surfaces in Arbitrary Motion." *Philosophical Transactions of the Royal Society of London Series A* 264 (May):321–42.
- Findlay, Charlotte R., Laia Rojano-Doñate, Jakob Tougaard, Mark P. Johnson, and Peter Teglberg Madsen. 2023. "Small Reductions in Cargo Vessel Speed Substantially Reduce Noise Impacts to Marine Mammals." *Science Advances* 9 (25): eadf2987. <https://doi.org/10.1126/sciadv.adf2987>.
- Foeth, E.J., and M. Deij-van Rijswijk. 2019. "Remodelling the B-Series Geometry in a CAD Environment." In *Sixth International Symposium on Marine Propulsors (SMP'19)*. Rome, Italy.
- ISO. 2017. "18405:2017(E) Underwater Acoustics - Terminology." Geneva, Switzerland.
- ISO. 2019. "17208-2:2019*(E) Underwater Acoustics — Quantities and Procedures for Description and Measurement of Underwater Sound from Ships — Part 2: Determination of Source Levels from Deep Water Measurements." Geneva, Switzerland.
- Lafeber, F H, J Bosschers, E van Wijngaarden, T Lloyd, and A Lidtke. 2020. "Development of Cavitation-Related Underwater Radiated Noise Prediction Models." Technical report NAVAIS project report Annex B to deliverables D4.3 and D4.4. Wageningen, the Netherlands: Maritime Research Institute Netherlands.
- Lafeber, Frans Hendrik, Johan Bosschers, Artur Lidtke, Thomas Lloyd, Erik van Wijngaarden, and Joost Moulijn. 2022. "Prediction of Underwater Radiated Noise from Propeller Cavitation during Concept Design." In *Proceedings of 7th Symposium on Marine Propulsors*. 17th-21st October, Wuxi, China.
- Lloyd, Thomas, Johanna Marie Daniel, Johan Bosschers, and Max G. Schuster. 2024. "'PIANO': A Physics-Based Semi-Empirical Source Level Model for Fleet-Scale Ship URN Prediction," April. <https://doi.org/10.15480/882.9335>.
- Lloyd, Thomas, Evert-Jan Foeth, Frans Hendrik Lafeber, Johan Bosschers, Yvette Klinkenberg, Miloš Birvalski, Levent Kaydihan, Artur Lidtke, and Erik van Wijngaarden. 2024. "Mitigation of Ship Underwater Radiated Sound by Propeller Optimisation and Bubble Injection." Technical report Saturn D4.3. Maritime Research Institute Netherlands.
- MacGillivray, Alexander, and Christ De Jong. 2021. "A Reference Spectrum Model for Estimating Source Levels of Marine Shipping Based on Automated Identification System Data." *Journal of Marine Science and Engineering* 9 (4): 369. <https://doi.org/10.3390/jmse9040369>.
- MacGillivray, Alexander O., Zizheng Li, David E. Hannay, Krista B. Trounce, and Orla M. Robinson. 2019. "Slowing Deep-Sea Commercial Vessels Reduces Underwater Radiated Noise." *The Journal of the Acoustical Society of America* 146 (1): 340–51. <https://doi.org/10.1121/1.5116140>.

- Quiet Sound programme. 2024. "Results of 2023-2024 Voluntary Commercial Vessel Slowdown in Washington Waters for the Protection of Southern Resident Killer Whales." Washington Maritime Blue.
- SDC 9/INF.11. 2022. "Study on Comparison of Operational and Design Approaches Based on the Relationship between Underwater Radiated Noise (URN) Reduction Measures and GHG Emission." SDC 9/INF.11. International Maritime Organization.
- Sederberg, T.W. 2016. *Computer Aided Geometric Design*.
- Valentine, T. 1974. "The Effect of Nose Radius on the Cavitation-Inception Characteristics of Two-Dimensional Hydrofoils." AD-785 834. Naval Ship Research and Development Center.
- Vancouver Fraser Port Authority. 2023. "2023 Annual Report."
- Vaz, G., and J. Bosschers. 2006. "Modelling Three-Dimensional Sheet Cavitation on Marine Propellers Using a Boundary Element Method." In . Wageningen, Netherlands.
- Zhang, X, X Zheng, R Cheng, J Qiu, and Y Jin. 2018. "A Competitive Mechanism Based Multi-Objective Particle Swarm Optimiser with Fast Convergence." *Information Sciences* 427:63–76.

